ACS APPLIED MATERIALS & INTERFACES

Research Article

Cite This: ACS Appl. Mater. Interfaces 2018, 10, 34664−34673

www.acsami.org

Nature-Inspired Hydrogels with Soft and Stiff Zones that Exhibit a 100-Fold Difference in Elastic Modulus

Salimeh Gharazi,[†] Brady C. Zarket,[†] Kerry C. DeMella, and Srinivasa R. Raghavan*

Department of Chemical & Biomolecular Engineering, University of Maryland, College Park, Maryland 20742, United States

Supporting Information

ABSTRACT: Many biological materials, such as the squid beak and the spinal disc, have a combination of stiff and soft parts with very different mechanical properties, for example, the elastic modulus (stiffness) of the stiffest part of the squid beak is about 100 times that of the softest part. Researchers have attempted to mimic such structures using hydrogels but have not succeeded in synthesizing bulk gels with such large variations in moduli. Here, we present a general approach that can be used to form hydrogels with two or more zones having appreciably different mechanical characters. For this purpose, we use a technique developed in our lab for creating hybrid hydrogels with distinct zones. For the soft zone of the gel, we form a polymer network using a conventional acrylic monomer [*N*,*N*′-dimethylacrylamide (DMAA)] and with laponite (LAP) nanoparticles as the cross-linkers. For the stiff zone, we combine DMAA, LAP, and a methacrylated silica precursor ([3-(methacryloyloxy)-propyl]trimethoxy-silane). When this mixture is polymerized, nanoscale silica particles (~300 nm in diameter) are formed, and these serve as additional cross-links between the polymer chains, making this network very stiff. The unique character of each zone is preserved in the hybrid gel, and different zones are covalently linked to each other, thereby ensuring robust interfaces. Rheological measurements show that the elastic modulus of the stiff zone can be more than 100 times that of the soft zone. This ratio of moduli is the highest reported to date in a single, continuous gel and is comparable to the ratio in the squid beak. We present different variations of our soft−stiff hybrid gels, including multizone cylinders and core−shell discs. Such soft−stiff gels could have utility in bioengineering, such as in interfacing stiff medical implants with soft tissues.

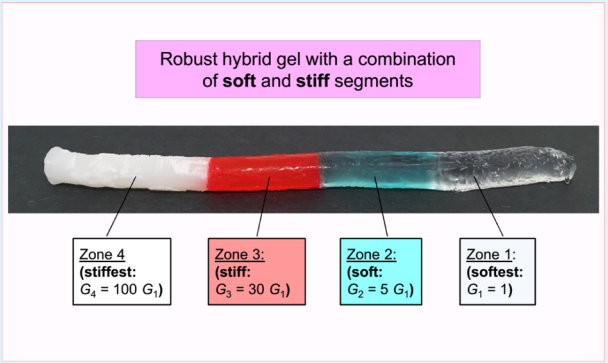

KEYWORDS: *hybrid, nanocomposite, silica nanoparticles, compressive modulus, shear modulus*

INTRODUCTION

Biological materials are frequently in a gel state, that is, they exhibit the properties of elastomeric solids while containing a large fraction of liquid (water) within them.[1−3] These include aquatic invertebrate animals like squids, octopuses, sponges, and jellyfish, as well as terrestrial invertebrates like worms and snails. Although these creatures may have hard or stiff elements within them, for the most part, they are soft and gel-like. In our bodies also, many tissues, organs, or other body parts are gel-like and compliant.[4,5] From the viewpoint of a materials engineer, such soft objects bring to mind polymer hydrogels, which are water-swollen networks of polymer chains cross-linked by chemical or physical bonds.[6−9] Hydrogels are easily formed in the lab by free-radical polymerization of monomers and cross-linkers. In recent years, researchers working on hydrogels have begun to recognize the remarkable properties of biological gels and attempted to mimic them. For example, gels with the mechanical resilience and toughness of cartilage[10] or the responsive properties of sea cucumbers[11] have been reported. One additional feature of biological gels is their hybrid or multisegmented nature.[12,13] That is, although a given gel may appear to be a single, homogeneous unit, it may actually have many connected segments. Individual segments may differ in their chemical or biochemical composition (i.e., each part may have its own type of cells or extracellular matrix) or in their micro- or nanostructure (e.g., cells may be oriented into chains in one segment but not others). These chemical or structural differences are often reflected in the macroscopic properties of the various segments, specifically their *mechanical* properties.

Two examples help to illustrate the mechanical differences within a biological soft material, and these are (a) the squid beak[14−16] and (b) the spinal disc.[4,5] Schematics of these structures are provided in Figure S1 (Supporting Information section.) Both of these are fully organic materials, that is, they do not contain inorganic minerals in them. Yet, in the squid beak, the tip (rostrum) is very stiff, with an elastic modulus around 5 GPa, whereas the base is much softer, with a modulus around 50 MPa (Figure S1a). Thus, the ratio in moduli between the stiff and soft ends is about 100. Between these

Received: August 16, 2018
Accepted: September 17, 2018
Published: September 28, 2018

Downloaded via UNIV OF MARYLAND COLG PARK on October 20, 2018 at 11:07:24 (UTC).
See https://pubs.acs.org/sharingguidelines for options on how to legitimately share published articles.

© 2018 American Chemical Society

DOI: 10.1021/acsami.8b14126
ACS Appl. Mater. Interfaces 2018, 10, 34664−34673

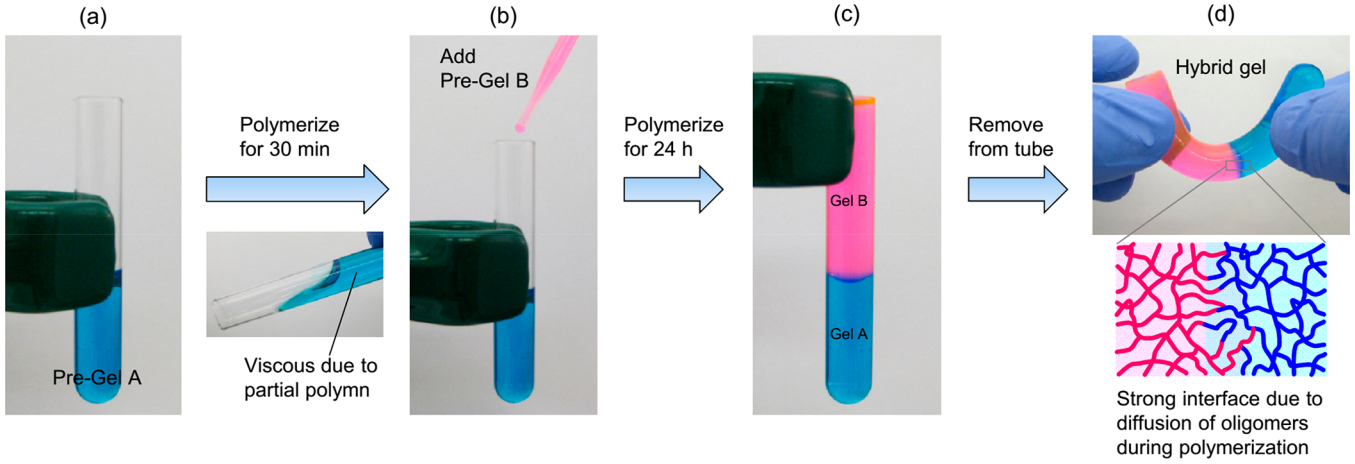

Figure 1. Procedure for preparing hybrid gels with mechanically distinct zones. The schematics show the preparation of a cylindrical hybrid with two zones, gel A and gel B. The pregels corresponding to the two zones (mixtures of monomer, cross-linker, initiator, and accelerant) are colored with a blue and a pink dye, respectively. (a) Pregel A is placed in a tube and polymerized for a short time until the sample becomes viscous. (b) Pregel B is then added slowly on top of pregel A. Because of the high viscosity of pregel A, there is no convective mixing at the interface. (c) The combination is then polymerized, whereupon a hybrid gel with distinct gel A and gel B zones is formed. (d) The hybrid is then removed from the tube, and it is revealed to be a robust material with a strong interface. The schematic shows that the interface is strengthened by the diffusion of oligomers into their adjacent zones during polymerization.

extremes, there exist mechanically distinct zones (Figure S1a). The mechanical differences are clearly related to function, that is, the hard and sharp tip enables tearing of food, whereas the softer base facilitates attachment to the rest of the squid. The differences in modulus (stiffness) arise because of differences in cross-link density and polymer concentration.[14−16] The tip of the beak is a highly cross-linked network of chitin fibers, catechols, and proteins, which together constitute ∼85% of the material (the remaining 15% is water). The base has mostly the same contents but at a much lower concentration (∼30%) and also a lower cross-link density. In the case of the spinal discs, which are located between consecutive vertebrae in the spine, there exist two segments or zones (Figure S1b): a soft, compliant core (*nucleus pulposus*, NP) surrounded by a stiff outer shell (*annulus fibrosus*, AF).[4,5] Both zones contain a proteoglycan gel and collagen fibrils. The AF has a higher concentration of these moieties, and the collagen fibrils in it are arranged in concentric lamellae. In healthy adults, the shear modulus of the AF is around 100 kPa and of the NP is ca. 10 kPa, meaning a modulus ratio of about 10 between the two.[5] This ratio is believed to decrease with age.[17] The core−shell design of the discs is believed to be important for proper functioning of the spine, that is, for supporting different types of mechanical stresses.[5,17]

Several researchers have attempted to create mimics of the squid beak[18−20] and of the spinal disc.[21−23] In the case of the squid beak, the focus has been on creating a hydrogel with a smooth mechanical gradient from one end to the other. The gradient is typically created by varying the cross-link density either between polymeric moieties or between nanoscale fillers embedded in the matrix. For example, Rowan et al.[18] reported a squid beak-inspired gradient film that had a ratio in elastic modulus between the stiff and soft ends of about 5. Other researchers have also created gels with mechanical gradients, with one popular method being the UV-irradiation of a photo-cross-linkable gel through a grayscale mask.[24−27] However, the maximum extent of these gradients, in terms of the modulus ratio between the stiffest and softest ends, is typically <10 and at most ∼50. Apart from smooth gradients, there have only been a few attempts to create gels with mechanically distinct zones.[28−32] In the case of spinal-disc-mimics, the focus has been on mimicking the AF or the NP alone, not on combining two such zones into the same material.[21−23] Note that if a gel had a smooth mechanical gradient, there would be no sharp interfaces in it; however, if there were two zones, a distinct interface would exist at which there would be an abrupt change from one material property to another.[28] *Such interfaces tend to be the weak points in a hybrid material, that is, the point at which the material fails when deformed.* This is one reason that researchers have preferred to make gradient materials over ones with zones. Thus, the challenge in creating multizone hydrogels is to ensure strong, robust interfaces between the zones.

Here, we present a general approach that can be used to form hydrogels with two or more zones having significantly different mechanical properties. We term these "soft−stiff" gels, and we show that the soft and stiff zones can exhibit a *100-fold difference* in elastic modulus (stiffness) measured under shear. The gel is robust enough that it can be picked up by hand and manipulated as a single object. *Moreover, when the gel is deformed, the interface between the zones remains robust and the gel does not break at the interface.* The strong interface is a consequence of the technique we use for creating hydrogels with dissimilar zones (Figure 1), which was developed previously in our lab[28] and has subsequently been copied and extended by others.[31,32] In preparing our hybrid, we were careful about the formulation chosen for each zone. We did not want the soft zone to be too soft as to be floppy or gooey, which is the case in gels made with very low cross-link densities. Such gels will then be incapable of being gripped or pulled by one's fingers. Conversely, we did not want the stiff zone to be brittle or fragile. Here again, if a very high cross-link density is used, a stiff gel can obtained, but this will tend to break easily, that is, it will not be strong or tough. *Our goal, instead, was to ensure that both the soft and stiff zones in the hybrid were independently firm and strong and that the overall gel was also robust.* These criteria are met by the gels described in the next section. The key is to use two different kinds of

DOI: 10.1021/acsami.8b14126
ACS Appl. Mater. Interfaces 2018, 10, 34664−34673

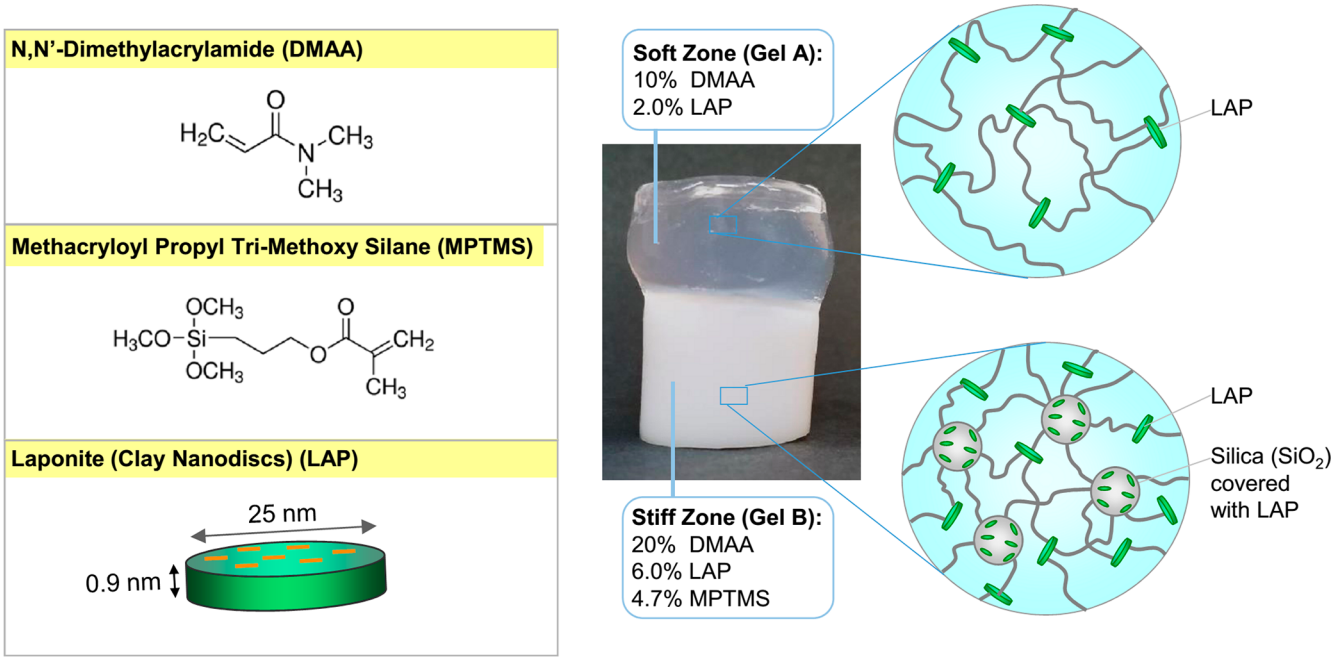

Figure 2. Components used to prepare the soft–stiff hybrid gel and the microstructure of each zone. The main components are the organic monomer *N,N′*-dimethylacrylamide (DMAA), the organic–inorganic monomer [3-(methacryloyloxy)-propyl]trimethoxy-silane (MPTMS), and the inorganic LAP particles. The soft zone is formed by polymerizing a mixture of DMAA and LAP, and it is clear or slightly translucent. The LAP particles act as cross-linkers for the DMAA chains, as shown by the schematic. The stiff zone is formed by polymerizing higher concentrations of DMAA and LAP, along with MPTMS. MPTMS initially forms insoluble droplets, which are stabilized by the adsorption of LAP particles on the droplet surfaces. With time, the droplets get converted into silica particles, and as a result, this zone appears opaque and white. Both the silica and the LAP particles act as cross-linkers for the polymer chains, as shown by the schematic. The methacrylate moieties on the silica particles allow the particles to connect to multiple polymer chains. The high stiffness of this zone is due to the higher density of cross-links as well as the multifunctional nature of the silica cross-links.

nanoparticles as the cross-linking nodes: for the soft zone, we use laponite (LAP), which is a type of synthetic clay,[33] and for the stiff zone, we use both LAP and in situ-generated silica nanoparticles.

RESULTS AND DISCUSSION

Gel Synthesis. Our method for preparing hybrid gels is illustrated in Figure 1. The key to this method is to bring pregel solutions into contact when their viscosities are sufficiently high to prevent convective mixing.[28] We first introduce pregel A (a mixture of monomer A, cross-linker, initiator, and accelerant) into a tube at room temperature, as shown in Figure 1a. Then, we let this polymerize for around 30 min. The monomers will be partially polymerized into oligomers or three-dimensional clusters, making the solution viscous (Figure 1b). Next, pregel B (a mixture of monomer B, cross-linker, initiator, and accelerant) is introduced on top of pregel A (Figure 1c). The high viscosity of pregel A will prevent convective mixing at the interface between the two pregels. We then let the whole system polymerize over 24 h. The final hybrid gel will have well-defined gel A and gel B zones and a strong interface between the zones (Figure 1d). Note that this method is widely applicable and it works regardless of the chemistry chosen for the two gels. For clarity, in Figure 1, we have included a blue dye (methylene blue) in gel A and a pink dye (rhodamine B) in gel B. Figure 1d shows that the two dyes remain within their respective zones even after polymerization. The inset shows that at the interface between the two zones (A and B), there is some interpenetration of the chains. That is, during polymerization, chains (oligomers) of A diffuse into zone B and vice versa. *As a result, there will be some covalent linkages of A and B chains at the interface, which is crucial in ensuring that the interface remains strong.*[28]

We used the above method to make a soft–stiff hybrid gel, that is, with soft and stiff zones. Figure 2 shows the components of each zone (all concentrations are in wt % relative to water). The soft zone (gel A) is made using the monomer DMAA (10%) and with LAP particles (2%) as the cross-linkers.[28,34] Why use LAP instead of a bifunctional cross-linker like *N,N′*-methylene-bis(acrylamide) (BIS)? If BIS is used at a low level, the gel obtained is very loose and floppy, which as noted above was not our intent. If a very high level of BIS is used, the gel will tend to be quite brittle and not very stretchable.[9,28] The advantage of LAP is that it gives rise to gels that are soft and yet flexible, stretchable, and strong.[28,34,35] Note that a DMAA-LAP gel is only formed when the two are combined with a free-radical initiator [in our case, it is ammonium persulfate (APS)] and made to undergo polymerization.[34] (i.e., a gel is not obtained if LAP particles are added after DMAA is polymerized.) When DMAA and LAP are in the presence of free radicals, polymer chains of DMAA are expected to grow from the surfaces of LAP particles, that is, the particles are expected to act as chemical cross-linkers for the polymer chains,[34] as shown by the schematic in Figure 2.

For the stiff zone (gel B), we combine higher concentrations of DMAA (20%) and LAP (6%), along with the methacrylated silane, MPTMS, (4.7%).[36−38] MPTMS is known to be a water-insoluble silica precursor that can form an emulsion when combined with water along with a stabilizer. It is also known

DOI: 10.1021/acsami.8b14126
ACS Appl. Mater. Interfaces 2018, 10, 34664−34673

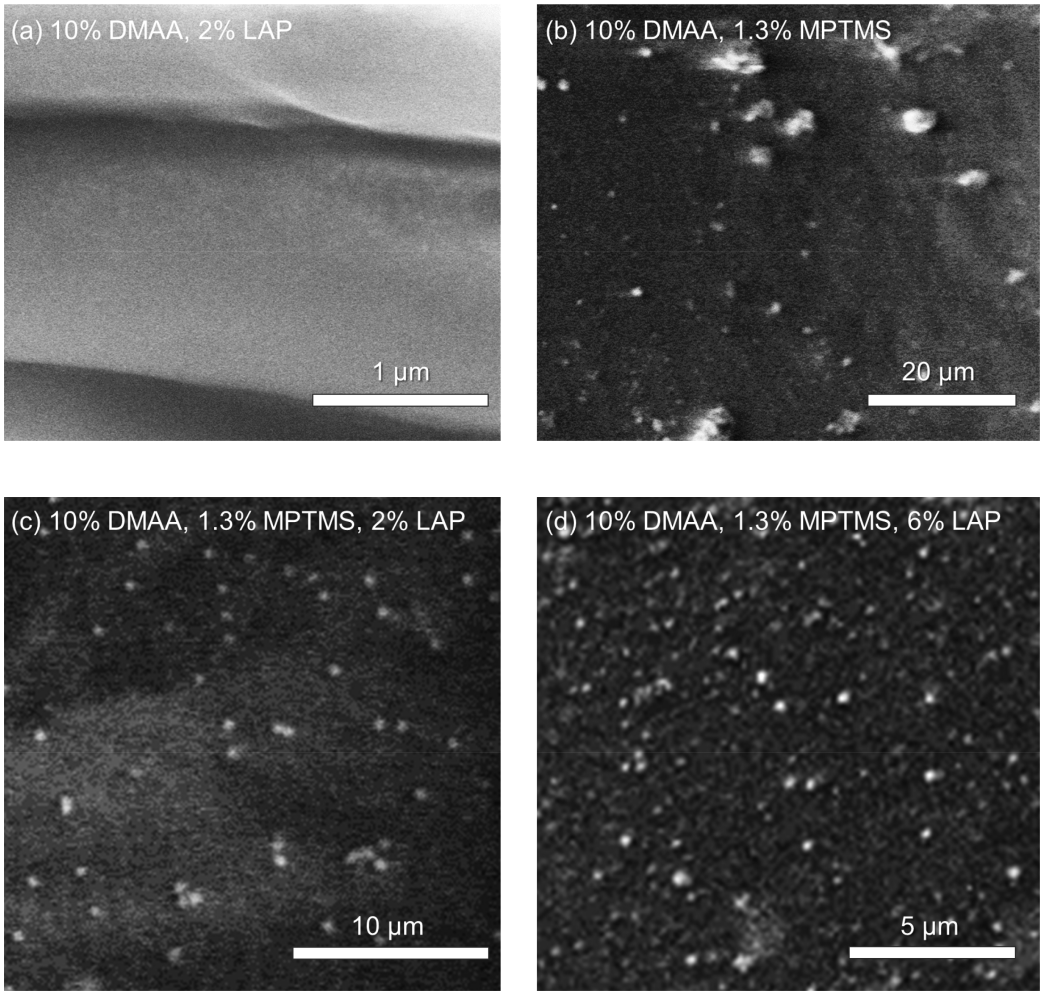

Figure 3. Microstructure of the gels, as revealed by SEM. (a) Gel of DMAA/LAP shows a smooth texture. The LAP discs are too thin to be observed in these images. (b) Gel of DMAA/MPTMS (no LAP) shows clusters of silica particles. (c,d) Gels formed by DMAA/MPTMS/LAP are seen to contain discrete silica particles. The particles have an average diameter of 500 nm in (c), where LAP is 2%, and an average diameter of 300 nm in (d), where LAP is 6%. The images indicate that LAP is necessary to form discrete silica particles of controlled size.

that LAP particles can stabilize the droplets in the emulsion, thereby forming a Pickering emulsion (i.e., the LAP particles are adsorbed onto the surfaces of the droplets).[39] Thus, in a pregel B sample (mixture of DMAA, LAP, and MPTMS, along with initiator), we initially have stable nanoscale droplets of MPTMS, and the sample is cloudy. Over time (within ~30 min), the mixture becomes much more turbid, indicating that MPTMS in the droplets is getting hydrolyzed and thereafter condensing to form silica (SiO_2) nanoparticles.[40] At this point, the sample viscosity is still low, which means that the particles form well before the polymerization is complete. Next, the methacrylate groups on MPTMS molecules at the particle surfaces will be able to copolymerize with DMAA.[36] The silica particles will then act as multifunctional cross-links for the polymer chains,[36,40] thereby increasing the connectivity of the network. In other words, there will be a combination of cross-links (nodes or junctions) in gel B because of both the LAP nanoparticles and the silica nanoparticles, as shown by the schematic in Figure 2. Silica, in particular, will be connected to numerous polymer chains at the same time. This is the main reason for the higher stiffness of gel B.

The rationale for using MPTMS for the stiff zone can be further explained as follows. Generally, a stiff gel requires a higher density of cross-links, which could be achieved in our system by (a) increasing the concentration of the monomer (DMAA), (b) increasing the concentration of the cross-linker (LAP), or (c) increasing the *functionality* of the cross-linkers (LAP + MPTMS). Our focus is on (c). Gels have been formed by other researchers with LAP as high as 20%, and this alone can be enough to increase the gel modulus to the kPa range.[35] However, LAP particles tend to form a physical gel in water even at around 2% (the particles are initially well-dispersed but assemble into a gel over time).[33] Thus a monomer solution with 20% LAP is difficult to prepare and work with.[35] For comparison, at ~ 2 to 6% LAP, the solution is initially of low viscosity and it takes several hours to form a physical gel. Thus, in our studies, we chose to have both the soft and stiff zones made with moderate DMAA and LAP content. The main difference is that there is ~5% MPTMS in the stiff zone, and this is enough to dramatically raise the modulus of this gel, while keeping it strong and robust.

Gel Microstructure. We used scanning electron microscopy (SEM) to study the above gels. SEM micrographs are shown in Figure 3 for a series of gels, all containing 10% DMAA. The gel with 10% DMAA and 2% LAP (no MPTMS) shows a smooth texture (Figure 3a), indicating its homogeneous nature. Note that the LAP particles, which are discs of diameter 25 nm and thickness 1 nm (see Figure 2), are too

DOI: 10.1021/acsami.8b14126
ACS Appl. Mater. Interfaces 2018, 10, 34664−34673

small to be resolved by SEM. The homogeneous microstructure of DMAA/LAP gels is also consistent with their visual transparency, as seen for the gel A zone in Figure 2. In contrast, all of the gels prepared with MPTMS reveal the presence of silica particles under SEM, which are seen as white structures in Figure 3b–d. The presence of particles in these gels is also consistent with visual observation because these gels are seen to be whitish and opaque (Figure 2). Energy-dispersive X-ray (EDX) analysis in SEM (see Figure S2, Supporting Information) also confirmed the elemental composition to be Si and O at the locations of the particles, indicating the particles to be silica. This is consistent with previous studies that have used MPTMS as a silica precursor, either in water or in a polymeric matrix.[36,38]

Next, we focus on the differences in microstructure between the various gels in Figure 3b–d. For the gel with DMAA and 1.3% MPTMS (no LAP), the silica particles are clustered into large microscale units (Figure 3b). Image analysis was used to determine the cluster sizes in Figure 3b. The clusters span a wide distribution in size, with their average diameter being around 3 μm. For the gel with 1.3% MPTMS and 2% LAP (Figure 3c), the silica particles are discrete (not clustered) and are distributed uniformly in the sample. From image analysis, we determine the average diameter of the particles to be around 500 nm. Similarly, for the gel with 1.3% MPTMS and 6% LAP (Figure 3d), the silica particles are discrete and a bit smaller, with an average diameter around 300 nm.

The above results indicate that the LAP particles help to control the size and stability of silica in the DMAA/MPTMS/LAP gels. In the absence of LAP, the silica particles are clustered. However, incorporation of LAP ensures that the silica particles stay discrete, and the higher the LAP, the smaller the silica. The likely reason for these results, based on the literature, is that a Pickering emulsion (i.e., a particle-stabilized emulsion) is expected to form in mixtures of MPTMS and LAP.[37,38] That is, the MPTMS droplets in water are expected to be stabilized by the adsorption of LAP particles onto the droplet surfaces. Adsorption of LAP discs onto the droplets occurs due to the interfacial activity of LAP and is not simply due to charge.[33,39] The droplets eventually convert into silica particles, and thus, when the droplets are small, the silica particles in the final cross-linked gel are also small. In turn, when the silica particles are small and unclustered, the mechanical properties of the gel are much improved. Indeed, we find from our studies that DMAA/MPTMS gels without LAP are inhomogeneous (because of the presence of silica clusters, see Figure 3b) and as a result tend to rupture easily under moderate deformations (i.e., are quite brittle). This is because the silica clusters will act as "defects", that is, points where the stress will be concentrated, causing the sample to fail. However, the incorporation of LAP gives rise to gels that are both very stiff as well as strong and fracture-resistant. This is further discussed below.

Mechanical Properties. We now discuss the mechanical response of our soft–stiff hybrid gels under three modes of deformation: tension, compression, and shear. First, the behavior under tension is shown visually in Figure 4. The initial hybrid gel is a cylinder of diameter 6 mm, with the soft and stiff zones each having a length of 24 mm (Figure 4a). The soft zone is clear and has a composition of 10% DMAA and 2% LAP. The stiff zone is opaque (white) and is made from 20% DMAA, 6% LAP, and 4.67% MPTMS. The hybrid gel is gripped on each end by the student's fingers and stretched

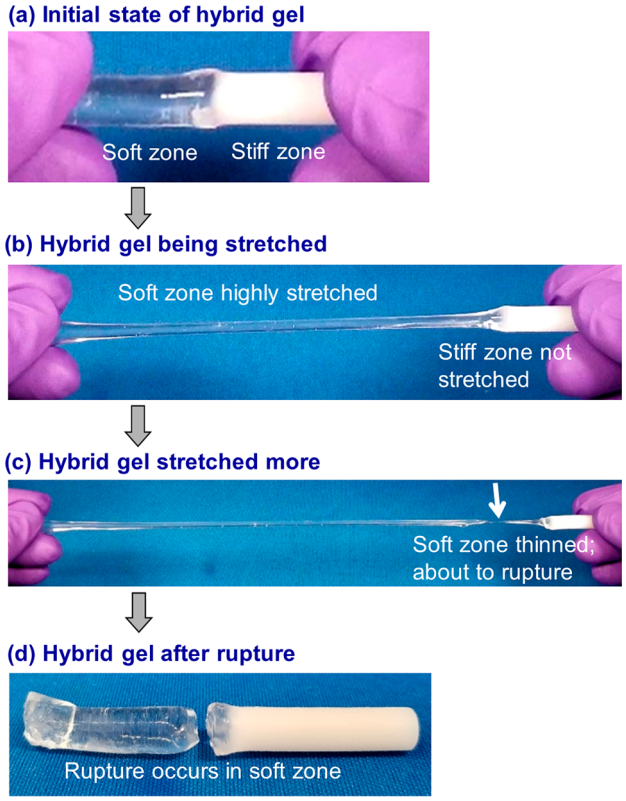

Figure 4. Photos showing the tensile properties of the soft–stiff hybrid gels. The initial hybrid gel (a) has equal lengths (24 mm each) of its soft (clear) and stiff (white) zones. When stretched (b,c), the soft zone expands to about 10 times its original length, whereas the stiff zone hardly changes its dimensions. The gel finally ruptures at a point within the soft zone (c,d). Note that the gel does not rupture at the interface between the zones.

axially. The soft zone gets stretched up to about 10 times its initial length (1000% strain), and in the process, this zone becomes a much thinner cylindrical filament (Figure 4b,c). The stiff zone, however, is stretched negligibly compared to its original dimensions. This indicates that the stiff zone has a much higher tensile modulus than the soft zone. As the stretching is continued, the gel eventually fails, but this failure occurs within the highly stretched soft zone (Figure 4c,d) while the stiff zone remains intact. Also, importantly, failure does not occur at the interface, indicating a strong interfacial connection between the soft and stiff zones. The strong interface is a consequence of using the method shown in Figure 1 to prepare the hybrid gel.[28]

Next, we evaluate the soft–stiff hybrid under compression. For this, we used a cylindrical gel with a diameter of 26 mm, with the soft and stiff zones each having a height of 21 mm (Figure 5a). The compositions of the soft and stiff zones are identical to those in Figure 4. In Figure 5b,c, a metal object is placed on the gel and a compressive force is applied downward. The soft zone gets compressed to about a third of its original height, causing this zone to expand laterally and protrude outward. The stiff zone, on the other hand, is hardly changed in its dimensions. Similar results are obtained if the soft zone is at the bottom of the hybrid (Figure 5b) or at the top (Figure 5c). Thus, visual observations again show the large difference in compressive modulus between the soft and stiff zones.

We proceeded to quantify the above differences using a rheometer. For this, gel cubes (length 4–10 mm) correspond-

DOI: 10.1021/acsami.8b14126
ACS Appl. Mater. Interfaces 2018, 10, 34664–34673

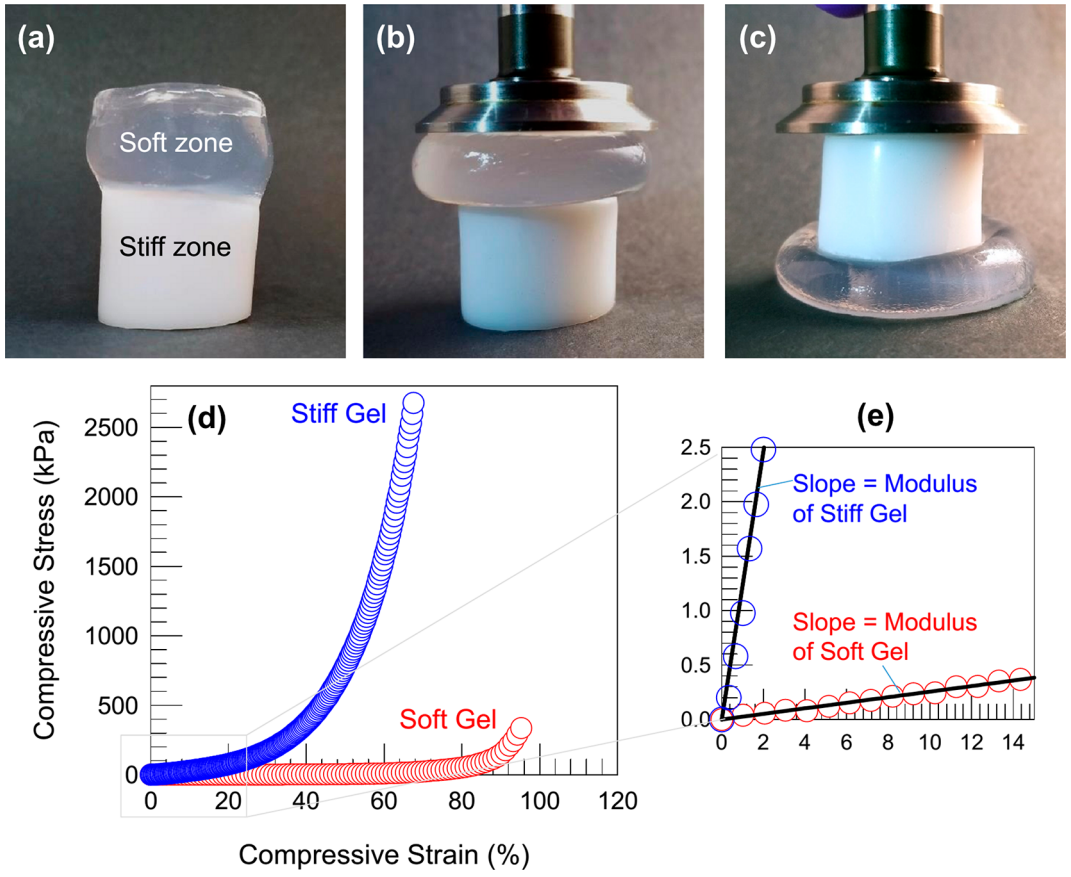

Figure 5. Photos and data showing the behavior of the soft−stiff hybrid gels under compression. The initial hybrid (a) is a cylinder with a diameter of 26 mm and with the soft zone (clear) and stiff zone (white) each having a height of 21 mm. When compressed manually (b,c), the soft zone is compressed by >60%, whereas the stiff zone is relatively unchanged in dimension. (d) Plot of compressive stress vs compressive strain for the soft and stiff zones. The inset in (e) shows the initial linear regions of the two curves, the slopes of which yield the compressive modulus of each gel. The compressive modulus of the stiff zone is ∼50 times that of the soft zone.

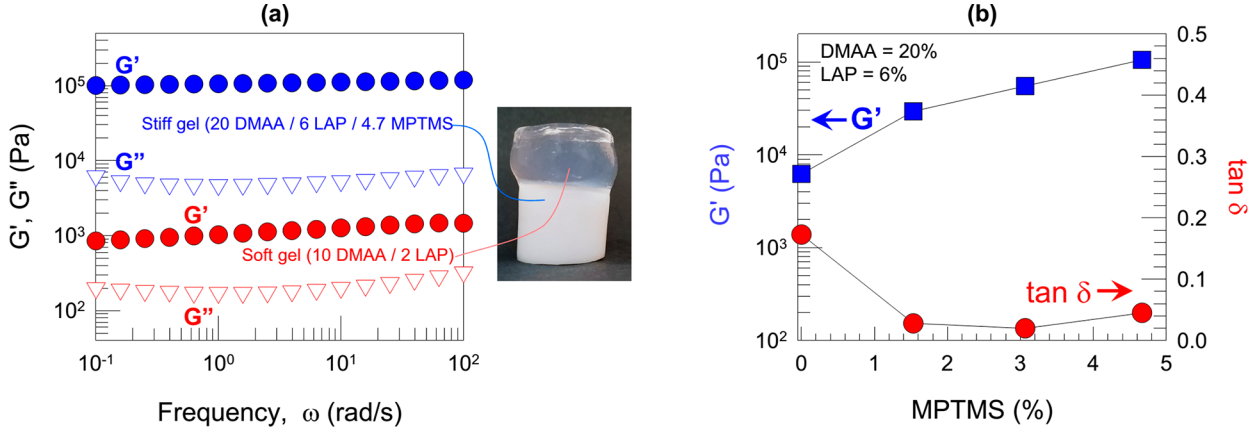

Figure 6. Oscillatory shear rheology of different zones of the soft−stiff hybrid gel. (a) The elastic modulus G' and the viscous modulus G'' are plotted as functions of the frequency ω for the soft and stiff zones of the hybrid. (b) G' and the loss tangent tan δ are plotted as a function of MPTMS content for DMAA/LAP/MPTMS gels, with DMAA held constant at 20% and LAP at 6%.

ing to the soft and stiff zones were prepared with the same compositions as in Figure 5a. The gels were then placed between the plates of a rheometer and compressed at a strain rate of 10%/min.[41,42] The compressive stress was measured, and this is plotted against the compressive strain in Figure 5d for the soft and stiff gels. As expected, a much higher stress is required to compress the stiff gel to a given strain compared to the soft gel. Figure 5e shows the initial regions of the two plots, and we have extracted the compressive moduli from the initial slopes.[42] Their values are 123 kPa for the stiff gel and 2.55 kPa for the soft gel. Thus, the ratio in compressive modulus between the stiff and soft zones of the hybrid is about 50. Interestingly, neither gel was destroyed due to the applied compression. The soft gel could be compressed by 95% (i.e., to 1/20th its original thickness) without breaking. The stiff gel was also quite strong and could be compressed by nearly 70%

DOI: 10.1021/acsami.8b14126
ACS Appl. Mater. Interfaces 2018, 10, 34664−34673

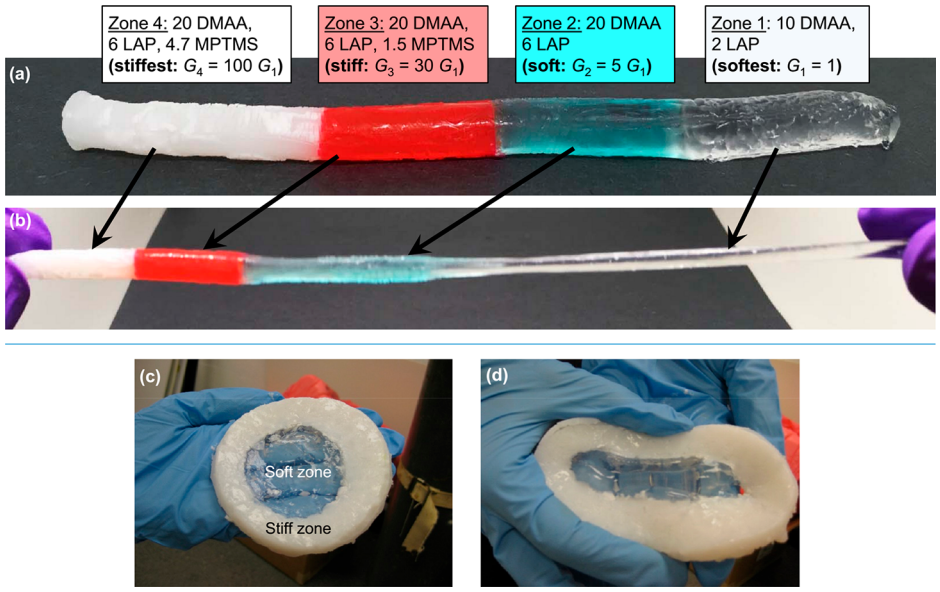

Figure 7. Variations of the soft–stiff hybrids: (a,b) multizone cylinders and (c,d) core–shell disks. (a) The gel has four zones, with zone 1 on the far right being the softest, with a shear modulus $G_1 \approx 1$ kPa and zone 4 on the far left having a modulus ~100 G_1. Between these, there are two more zones, each colored with a different dye and having intermediate moduli, as indicated. Zones 1 and 2 are prepared without MPTMS and are transparent, whereas zones 3 and 4 have MPTMS and are opaque. (b) The cylinder is stretched to show that zones 3 and 4 are negligibly extended, zone 2 is extended a bit, and zone 1 is extended a lot; this is also shown by Movie 1 (Supporting Information). (c) The disk has a soft core (DMAA/LAP, transparent) and a stiff shell (DMAA/MPTMS/LAP, opaque). (d) The disk is manually deformed to show the compliant nature of the core.

of its original thickness before the required force exceeded the limits of the instrument. Thus, the compressive strength of this gel exceeds 2.5 MPa (highest value on the *y*-axis in Figure 5d). Usually, stiff hydrogels made with high concentrations of cross-linkers tend to be very brittle and crumble into pieces when compressed.[43] However, the stiff zone of our hybrids shows an impressive combination of high modulus and high compressive strength.

Next, we studied the gels under oscillatory shear. These experiments were conducted on gel discs (diameter of 20 mm, height of 3–4 mm) corresponding to various compositions. Figure 6a shows the dynamic rheological response of the soft and stiff zones of the hybrid studied before in Figures 4 and 5. Both samples exhibit the characteristic rheological signature of gels, that is, their elastic modulus G' is much greater than their viscous modulus G'' and both G' and G'' are nearly independent of frequency.[44,45] The value of G' is the key parameter as it is the modulus (stiffness) of the gel under shear (in the linear viscoelastic region). For the stiff gel, G' is 105 kPa, whereas for the soft gel, G' is 1.03 kPa (both values correspond to a frequency of 1 rad/s). Thus, the ratio in elastic shear modulus between the stiff and soft gels is >100.

We have also systematically studied the mechanical properties as a function of MPTMS content. For these experiments, DMAA was held constant at 20%, LAP at 6%, and MPTMS was varied from 0 to 4.67%. Figure 6b shows data from dynamic rheology as a function of the MPTMS concentration. Two parameters are plotted: the elastic modulus G' and the loss tangent tan δ, which is the ratio of G'' to G'. As MPTMS in the gel increases, so does G', indicating that the gels become stiffer. Simultaneously, tan δ decreases, which implies that the gels become more solid-like. These data can be understood as follows. As MPTMS is increased, more silica particles will be formed, and because these act as multifunctional cross-links, the gel network will become much denser, which is reflected in a higher G'. Also, a denser network will tend to be more rigid, that is, there will be less viscous dissipation of the applied stress,[9,44] which explains the lowering of tan δ. If MPTMS is increased beyond 4.67% (for the above DMAA and LAP concentrations), the gels obtained are brittle and inhomogeneous, which is why no data are shown in the figure for such samples. This is likely because the LAP particles are required to form a stable Pickering emulsion of MPTMS, implying that the LAP/MPTMS ratio is important for stability.[38,39] If there is too much MPTMS, the droplets will be unstable and the silica particles that form will tend to cluster, as seen in Figure 3b.

Variations and Applications. We expect that there will be many potential applications for the soft–stiff hybrids described in this paper. To facilitate applications, it is useful to consider variations of the final material. For instance, in the squid beak (Figure S1a), one end is 100 times stiffer than the opposite end, and there are multiple zones between these extremes that ensure a gradual change in stiffness. Our synthesis scheme can be easily adapted to achieve such a material; specifically, we can have several zones instead of just two. As an example, Figure 7a,b show a cylinder with four distinct zones, with their compositions chosen based on Figure 6. The softest zone (zone 1) is the same as that in Figures 5 and 6a (10% DMAA, 2% LAP), and it has a shear modulus $G' \approx 1$ kPa. Zone 2 has 20% DMAA and 6% LAP and its $G' \sim 5$ kPa from Figure 6b. Zone 3 has 20% DMAA, 6% LAP, and 1.5% MPTMS and its $G' \approx 30$ kPa. Finally, zone 4, the stiffest zone, is made with 20% DMAA, 6% LAP, and 4.67% MPTMS and its $G' \approx 100$ kPa from Figure 6a. The four-zone cylinder was synthesized in the same way as our two-zone one, and we used a red dye (rhodamine 6G) in zone 3 and a blue-green dye (malachite green) in zone 2 to demarcate the zones. The zones thus have a relative stiffness of 100:30:5:1 from left to right

DOI: 10.1021/acsami.8b14126
ACS Appl. Mater. Interfaces 2018, 10, 34664–34673

(i.e., stiffest to softest) in Figure 7a. Each zone is ∼10 mm in length and the cylinder diameter is 5 mm.

In Figure 7b, this cylindrical gel is being stretched between a student's fingers. A video of this experiment is also provided as Movie 1 in the Supporting Information. We note that zones 4 and 3 are hardly extended relative to their initial dimensions, whereas zone 2 is stretched somewhat and zone 1 is stretched much more. The movie also reveals that when the stretching is stopped, the gel returns to its original dimensions, indicating elastic behavior. On the whole, the multizone cylinder exhibits a gradual step-down in mechanical stiffness from one end to another, and the more the zones, the more this will resemble a material with a smooth mechanical gradient.

Also, note from Figure 7a,b that there is hardly any leaching of the dye in zones 2 and 3 to their adjacent zones. This reflects the slow diffusion of dyes from one zone to another before and during polymerization, which as explained in Figure 1 is due to the high viscosities of each pregel (i.e., diffusivity varies inversely with solution viscosity.[45]). For this reason, each zone is well-defined both chemically and spatially, and there is a step-change in composition from one zone to another. However, if we deliberately wanted to create a smoother gradient, we could reduce the viscosities of the pregels at the instant they are brought into contact. There would then be some mixing between adjacent zones, and this would blur the edges of the zones in terms of composition. In turn, the mechanical properties would also change more gradually from one zone to another.

Last, we consider a concentric arrangement of the soft and stiff zones, similar to the spinal disc (schematic in Figure S1b). For this, we made a simple mold by combining two Petri dishes in a concentric fashion. The larger one had a diameter of 11 cm and the smaller one had a diameter of 5.4 cm. In the annular space between the two Petri dishes, we added pregel B corresponding to the stiff zone (20% DMAA, 6% LAP, and 4.67% MPTMS). After pregel B became viscous, we removed the inner Petri dish and added pregel A corresponding to the soft zone (10% DMAA, 2% LAP) in that space. Upon polymerization, we obtained the disclike hybrid shown in Figure 7c, which has a thickness (height) of 5 mm and an overall diameter of 11 cm. The core of this disc is the soft zone and it is transparent. The shell is the stiff zone, and it is white and opaque. Figure 7d shows that the hybrid can be squished and still retain its mechanical integrity. The core is compliant, whereas the shell is stiff and rigid, as is the case in the spinal disc.

CONCLUSIONS

We have demonstrated the synthesis of soft−stiff hybrid gels where there is a significant contrast in mechanical properties between the soft and stiff zones. Specifically, we have achieved a 100-fold difference in shear modulus and a 50-fold difference in compressive modulus between these zones. To our knowledge, this is the highest mechanical disparity engineered within a single polymeric material. It is interesting that a 100-fold difference in modulus is also seen between regions of the squid beak, which is a fully organic material that has served as a source of inspiration for this work. The key to our synthesis is the use of a methacrylated silane for the stiff zone of our hybrid gel. Silica nanoparticles are thus formed by a sol−gel process in the stiff zone, and these are connected to multiple polymer chains through covalent bonds at the particle surface. The multifunctional nature of the silica cross-links dictates the high modulus of this zone.

Despite the modulus mismatch between zones, our hybrid gel is a robust material. Both zones of the hybrid are firm and strong, and the overall gel can be gripped by hand and stretched. When the material breaks upon overstretching, failure occurs within a zone and not at the interface between the zones. This is a consequence of our synthesis method, which allows for strong, covalent connections to form at the interface between the polymers in each zone. We believe the hybrid gels engineered in this study will find many applications such as in tissue engineering. Moreover, when medical implants are placed in the body, these gels could be used to connect the implant to the underlying tissue. That is, the stiff portion of the gel could be interfaced with the implant, whereas the soft portion could help it anchor to the tissue.

MATERIALS AND METHODS

Materials. The monomers DMAA and MPTMS, the initiator APS, and the accelerator *N*,*N*,*N*′,*N*′-tetra-methylethylenediamine (TEMED) were purchased from Sigma-Aldrich. Laponite XLG nanoparticles (LAP) were a gift from Southern Clay Products.

Gel Preparation. All gels were prepared using deionized water that was degassed by exposure to nitrogen. The pregel (soft zone) was composed of DMAA and LAP, with typical concentrations of 10% DMAA (equivalent to 1 M) and 2% LAP. DMAA and LAP were combined under vigorous mixing using a stir bar. Pregel B (stiff zone) consisted of DMAA, LAP, and MPTMS, with typical concentrations being 20% DMAA, 6% LAP, and 4.67% MPTMS. To make this pregel, DMAA and LAP were mixed vigorously using a stir bar until the sample became homogeneous. Thereafter, MPTMS was added and the sample was sequentially mixed at higher shear using sonication (1 min) followed by vortex mixing (1 min) for a total of about 15 min until it appeared uniform and milky white. Both of these pregels had a low viscosity (akin to water) at this stage, and they were used to prepare the hybrid gels as indicated in Figure 1. Prior to introducing a given pregel into the container for making the hybrid, the initiator (150 μL of a 0.1% APS solution) and accelerator (30 μL of TEMED) were added and the mixture was vortexed. At this stage, the polymerization begins to occur at room temperature, and so, the pregels had to be quickly transferred to the container for gel preparation. Polymerizations were performed under a nitrogen atmosphere in a variety of containers (e.g., plastic tubes, vials, or Petri dishes). After polymerization, the final hybrid gel was removed from the container either by pushing it out or breaking the container.

Rheological Studies. All rheological experiments were run on an AR2000 rheometer (TA Instruments) at 25 °C using a parallel plate geometry (20 mm in diameter). For the oscillatory shear (dynamic rheology) experiments, gel samples were cut into discs of diameter 20 mm and thickness 3−4 mm. The linear viscoelastic region of each sample was obtained by stress-sweep experiments, and a strain within this region (typically 1%) was used to run the frequency-sweep experiments. Compression experiments were conducted using the squeeze-test mode.[41,42] Gel cubes (size from 4 to 10 mm) were placed at the center of the plates. Compression was performed at a rate of 10% strain per minute, which was determined based on the initial sample thickness. The normal-stress transducer was used to collect the normal force during compression, and this was converted to stress based on the initial surface area of the gel. This transducer had an upper limit of 50 N, and for the stiff gel, compression was stopped when the measured force approached this limit.

Scanning Electron Microscopy. A Hitachi SU-70 SEM was used to image the gels. For each gel, a small segment was cut and placed on double-sided carbon tape. A coating of Au/Pd was sputtered onto the gel surface prior to imaging. Accelerating voltages of 3.5 and 10 keV were used in the experiments. EDX spectrometry, using Bruker XFlash 4010 with a silicon drift detector, was performed on a portion of the sample to determine its elemental composition.

DOI: 10.1021/acsami.8b14126
ACS Appl. Mater. Interfaces 2018, 10, 34664−34673

■ ASSOCIATED CONTENT

Supporting Information

The Supporting Information is available free of charge on the ACS Publications website at DOI: 10.1021/acsami.8b14126.

Schematics of the squid beak and the spinal disc and SEM data analysis (PDF)

Movie showing extension of the multizone hybrid gel from Figure 7 (MPG)

■ AUTHOR INFORMATION

Corresponding Author

*E-mail: sraghava@umd.edu.

ORCID

Srinivasa R. Raghavan: 0000-0003-0710-9845

Author Contributions

†S.G. and B.C.Z. equally contributed to this work.

Notes

The authors declare no competing financial interest.

■ ACKNOWLEDGMENTS

We acknowledge the contributions of Stephen Banik and Neville Fernandes to some of the experiments described in this paper.

■ REFERENCES

(1) Alberts, B. *Molecular Biology of the Cell*, 4th ed.; Garland Publishers: New York, 2002.

(2) *OpenStaxCollege Biology* downloadable at: http://cnx.org/content/col11448/latest/, 2013.

(3) Levinton, J. S. *Marine Biology: Function, Biodiversity*; Ecology Oxford University Press: Oxford, 2014.

(4) Gray, H. *Anatomy of the Human Body*; Bartleby: New York, 2000.

(5) Adams, M. A. Intervertebral Disc Tissues. In *Mechanical Properties of Aging Soft Tissues*; Derby, B., Akhtar, R., Eds.; Springer: Switzerland, 2015; pp 7−35.

(6) Tanaka, T. Gels. *Sci. Am.* **1981**, *244*, 124−138.

(7) Osada, Y.; Gong, J. P.; Tanaka, Y. Polymer Gels. *J. Macromol. Sci., Polym. Rev.* **2004**, *44*, 87−112.

(8) Laftah, W. A.; Hashim, S.; Ibrahim, A. N. Polymer Hydrogels: A Review. *Polym.-Plast. Technol. Eng.* **2011**, *50*, 1475−1486.

(9) Cipriano, B. H.; Banik, S. J.; Sharma, R.; Rumore, D.; Hwang, W.; Briber, R. M.; Raghavan, S. R. Superabsorbent Hydrogels that are Robust and Highly Stretchable. *Macromolecules* **2014**, *47*, 4445−4452.

(10) Sun, J.-Y.; Zhao, X.; Illeperuma, W. R. K.; Chaudhuri, O.; Oh, K. H.; Mooney, D. J.; Vlassak, J. J.; Suo, Z. Highly Stretchable and Tough Hydrogels. *Nature* **2012**, *489*, 133−136.

(11) Capadona, J. R.; Shanmuganathan, K.; Tyler, D. J.; Rowan, S. J.; Weder, C. Stimuli-Responsive Polymer Nanocomposites Inspired by the Sea Cucumber Dermis. *Science* **2008**, *319*, 1370−1374.

(12) Bhushan, B. Biomimetics: lessons from nature-an overview. *Philos. Trans. R. Soc., A* **2009**, *367*, 1445−1486.

(13) Chen, P.-Y.; McKittrick, J.; Meyers, M. A. Biological Materials: Functional Adaptations and Bioinspired Designs. *Prog. Mater. Sci.* **2012**, *57*, 1492−1704.

(14) Miserez, A.; Li, Y.; Waite, J. H.; Zok, F. Jumbo Squid Beaks: Inspiration for Design of Robust Organic Composites. *Acta Biomater.* **2007**, *3*, 139−149.

(15) Miserez, A.; Schneberk, T.; Sun, C.; Zok, F. W.; Waite, J. H. The Transition from Stiff to Compliant Materials in Squid Beaks. *Science* **2008**, *319*, 1816−1819.

(16) Tan, Y.; Hoon, S.; Guerette, P. A.; Wei, W.; Ghadban, A.; Hao, C.; Miserez, A.; Waite, J. H. Infiltration of Chitin by Protein Coacervates Defines the Squid Beak Mechanical Gradient. *Nat. Chem. Biol.* **2015**, *11*, 488−495.

(17) Antoniou, J.; Epure, L. M.; Michalek, A. J.; Grant, M. P.; Iatridis, J. C.; Mwale, F. Analysis of Quantitative Magnetic Resonance Imaging and Biomechanical Parameters on Human Discs With Different Grades of Degeneration. *J. Magn. Reson. Imag.* **2013**, *38*, 1402−1414.

(18) Fox, J. D.; Capadona, J. R.; Marasco, P. D.; Rowan, S. J. Bioinspired Water-Enhanced Mechanical Gradient Nanocomposite Films That Mimic the Architecture and Properties of the Squid Beak. *J. Am. Chem. Soc.* **2013**, *135*, 5167−5174.

(19) Zvarec, O.; Purushotham, S.; Masic, A.; Ramanujan, R. V.; Miserez, A. Catechol-Functionalized Chitosan/Iron Oxide Nanoparticle Composite Inspired by Mussel Thread Coating and Squid Beak Interfacial Chemistry. *Langmuir* **2013**, *29*, 10899−10906.

(20) Zhang, X.; Hassanzadeh, P.; Miyake, T.; Jin, J.; Rolandi, M. Squid Beak Inspired Water Processable Chitosan Composites with Tunable Mechanical Properties. *J. Mater. Chem. B* **2016**, *4*, 2273−2279.

(21) Boelen, E. J. H.; van Hooy-Corstjens, C. S. J.; Bulstra, S. K.; van Ooij, A.; van Rhijn, L. W.; Koole, L. H. Intrinsically Radiopaque Hydrogels for Nucleus Pulposus Replacement. *Biomaterials* **2005**, *26*, 6674−6683.

(22) Nesti, L. J.; Li, W.-J.; Shanti, R. M.; Jiang, Y. J.; Jackson, W.; Freedman, B. A.; Kuklo, T. R.; Giuliani, J. R.; Tuan, R. S. Intervertebral Disc Tissue Engineering using a Novel Hyaluronic Acid−Nanofibrous Scaffold (HANFS) Amalgam. *Tissue Eng., Part A* **2008**, *14*, 1527−1537.

(23) Singha, K.; Singha, M. Biomechanism Profile of Intervertebral Discs (IVD): Strategies to Successful Tissue Engineering for Spinal Healing by Reinforced Composite Structure. *J. Tissue Sci. Eng.* **2012**, *3*, 118.

(24) Seidi, A.; Ramalingam, M.; Elloumi-Hannachi, I.; Ostrovidov, S.; Khademhosseini, A. Gradient Biomaterials for Soft-to-Hard Interface Tissue Engineering. *Acta Biomater.* **2011**, *7*, 1441−1451.

(25) Ross, A. M.; Lahann, J. Surface Engineering the Cellular Microenvironment via Patterning and Gradients. *J. Polym. Sci., Part B: Polym. Phys.* **2013**, *51*, 775−794.

(26) Chatterjee, K.; Lin-Gibson, S.; Wallace, W. E.; Parekh, S. H.; Lee, Y. J.; Cicerone, M. T.; Young, M. F.; Simon, C. G. The Effect of 3D Hydrogel Scaffold Modulus on Osteoblast Differentiation and Mineralization Revealed by Combinatorial Screening. *Biomaterials* **2010**, *31*, 5051−5062.

(27) Karpiak, J. V.; Ner, Y.; Almutairi, A. Density Gradient Multilayer Polymerization for Creating Complex Tissue. *Adv. Mater.* **2012**, *24*, 1466−1470.

(28) Banik, S. J.; Fernandes, N. J.; Thomas, P. C.; Raghavan, S. R. A New Approach for Creating Polymer Hydrogels with Regions of Distinct Chemical, Mechanical, and Optical Properties. *Macromolecules* **2012**, *45*, 5712−5717.

(29) Palleau, E.; Morales, D.; Dickey, M. D.; Velev, O. D. Reversible Patterning and Actuation of Hydrogels by Electrically Assisted Ionoprinting. *Nat. Commun.* **2013**, *4*, 2257.

(30) Tseng, H.; Cuchiara, M. L.; Durst, C. A.; Cuchiara, M. P.; Lin, C. J.; West, J. L.; Grande-Allen, K. J. Fabrication and Mechanical Evaluation of Anatomically-Inspired Quasilaminate Hydrogel Structures with Layer-Specific Formulations. *Ann. Biomed. Eng.* **2013**, *41*, 398−407.

(31) Yong, X.; Simakova, A.; Averick, S.; Gutierrez, J.; Kuksenok, O.; Balazs, A. C.; Matyjaszewski, K. Stackable, Covalently Fused Gels: Repair and Composite Formation. *Macromolecules* **2015**, *48*, 1169−1178.

(32) Beziau, A.; de Menezes, R. N. L.; Biswas, S.; Singh, A.; Cuthbert, J.; Balazs, A. C.; Kowalewski, T.; Matyjaszewski, K. Combining ATRP and FRP Gels: Soft Gluing of Polymeric Materials for the Fabrication of Stackable Gels. *Polymers* **2017**, *9*, 186.

(33) Cummins, H. Z. Liquid, Glass, Gel: The Phases of Colloidal Laponite. *J. Non-Cryst. Solids* **2007**, *353*, 3891−3905.

(34) Haraguchi, K. Stimuli-Responsive Nanocomposite Gels. *Colloid Polym. Sci.* **2011**, *289*, 455−473.

DOI: 10.1021/acsami.8b14126
ACS Appl. Mater. Interfaces 2018, 10, 34664−34673

(35) Haraguchi, K.; Li, H.-J. Mechanical Properties and Structure of Polymer−Clay Nanocomposite Gels with High Clay Content. *Macromolecules* **2006**, *39*, 1898−1905.
(36) Valliant, E. M.; Jones, J. R. Softening Bioactive Glass for Bone Regeneration: Sol-Gel Hybrid Materials. *Soft Matter* **2011**, *7*, 5083−5095.
(37) Guan, Y.; Meng, X.; Qiu, D. Hollow Microsphere with Mesoporous Shell by Pickering Emulsion Polymerization as a Potential Colloidal Collector for Organic Contaminants in Water. *Langmuir* **2014**, *30*, 3681−3686.
(38) Zhang, X.; Guan, Y.; Xie, Y.; Qiu, D. "House-of-cards" structures in silicone rubber composites for superb anti-collapsing performance at medium high temperature. *RSC Adv.* **2016**, *6*, 7970−7976.
(39) Cauvin, S.; Colver, P. J.; Bon, S. A. F. Pickering Stabilized Miniemulsion Polymerization: Preparation of Clay Armored Latexes. *Macromolecules* **2005**, *38*, 7887−7889.
(40) Brinker, C. J.; Scherer, G. W. *Sol-Gel Science: The Physics and Chemistry of Sol-Gel Processing*; Academic Press, 2013.
(41) White, J. C.; Saffer, E. M.; Bhatia, S. R. Alginate/PEO-PPO-PEO Composite Hydrogels with Thermally-Active Plasticity. *Biomacromolecules* **2013**, *14*, 4456−4464.
(42) Zarket, B. C.; Raghavan, S. R. Onion-Like Multilayered Polymer Capsules Synthesized by a Bioinspired Inside-Out Technique. *Nat. Commun.* **2017**, *8*, 193.
(43) Gong, J. P.; Katsuyama, Y.; Kurokawa, T.; Osada, Y. Double-Network Hydrogels with Extremely High Mechanical Strength. *Adv. Mater.* **2003**, *15*, 1155−1158.
(44) Macosko, C. W. *Rheology: Principles, Measurements, and Applications*; Wiley-VCH: New York, 1994.
(45) Larson, R. G. *The Structure and Rheology of Complex Fluids*; Oxford University Press: Oxford, 1999.

DOI: 10.1021/acsami.8b14126
ACS Appl. Mater. Interfaces 2018, 10, 34664−34673

Supporting Information for:

Nature-Inspired Hydrogels with Soft and Stiff Zones that Exhibit a 100-Fold Difference in Elastic Modulus

Salimeh Gharazi, Brady C. Zarket, Kerry C. DeMella and Srinivasa R. Raghavan*
Department of Chemical and Biomolecular Engineering, University of Maryland, College Park, MD 20742-2111
*Corresponding author. Email: sraghava@umd.edu

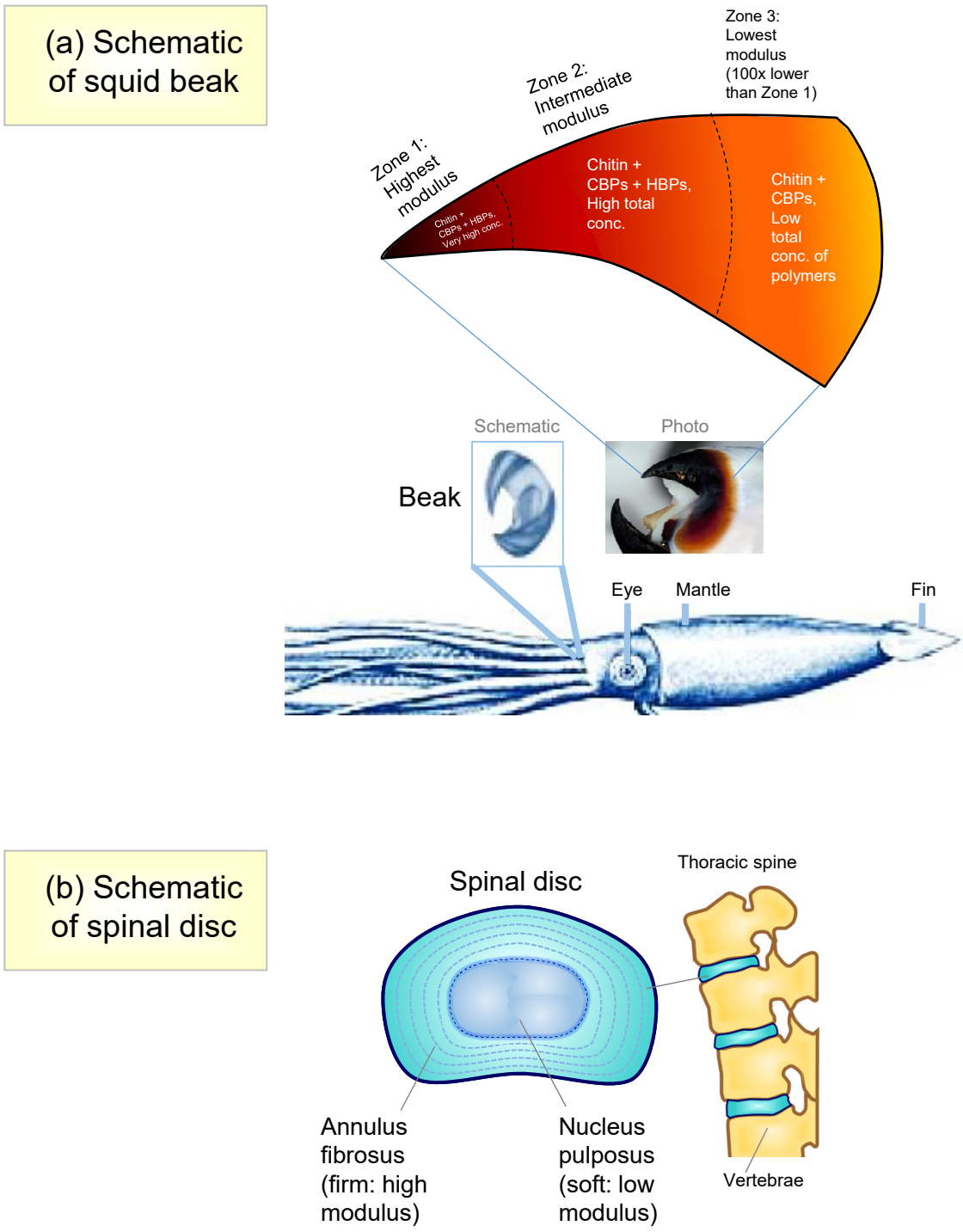

Figure S1. Two examples of natural structures that have parts or zones with different mechanical properties. (a) The squid beak, which is used by the squid to take in food. The location of the beak in the squid is indicated, and an overall schematic and photo of the beak are shown. A zoomed-in view of the beak reveals the gradation in stiffness (modulus) from the tip to the base. The beak can be broadly divided into three zones with differing composition (CBPs = chitin-binding proteins; HBPs = histidine binding proteins), which in turn dictates the stiffness of the zones. The zone near the tip is 100x stiffer than the base. (b) The spinal discs located between the vertebrae of the thoracic spine. The locations of the spinal discs in the vertebrae are indicated, and a zoomed-in top view of a single disc is shown schematically. The disc has a core-shell structure, with a soft core and a firm shell.

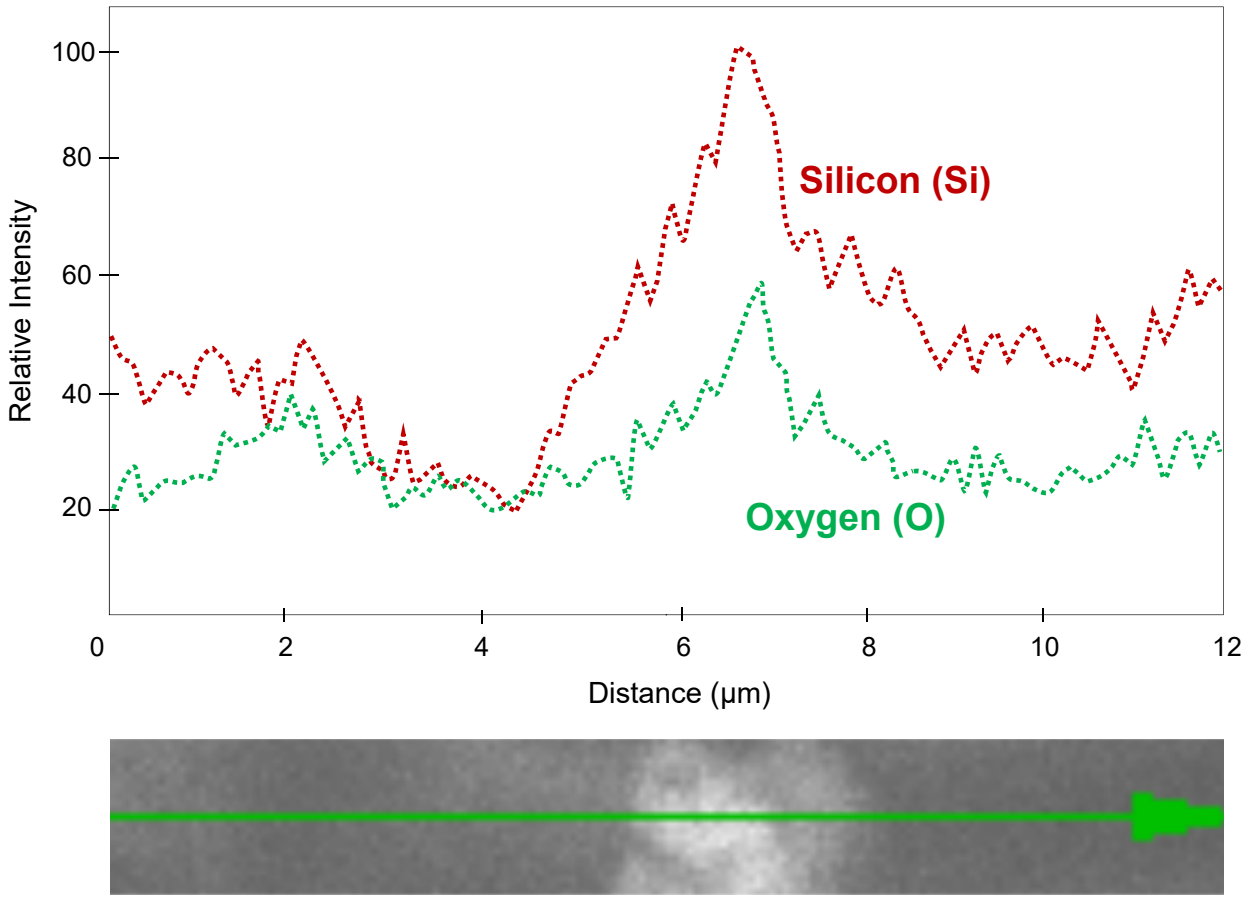

Figure S2. Elemental analysis using Energy-Dispersive X-Ray (EDX) of the particles in gels formed with MPTMS. A line scan is performed across a region in the SEM micrograph where a single particle is seen. The data show that the elements at the location of the particle are predominantly Si and O, indicating that the particle is silica (SiO_2)